6-16-2017

Emergence of dispersive shocks and rarefaction waves in power-law contact models

H. Yasuda
University of Washington

C. Chong
Bowdoin College

J. Yang
University of Washington

P. G. Kevrekidis
University of Massachusetts Amherst

Emergence of dispersive shocks and rarefaction waves in power-law contact models

H. Yasuda,[1] C. Chong,[2] J. Yang,[1,*] and P. G. Kevrekidis[3]
[1]*Aeronautics & Astronautics, University of Washington, Seattle, Washington 98195-2400, USA*
[2]*Department of Mathematics, Bowdoin College, Brunswick, Maine 04011, USA*
[3]*Department of Mathematics and Statistics, University of Massachusetts Amherst, Amherst, Massachusetts 01003-4515, USA*
(Received 1 December 2016; revised manuscript received 15 May 2017; published 16 June 2017)

In the present work, motivated by generalized forms of the Hertzian dynamics associated with granular crystals, we consider the possibility of such models to give rise to both dispersive shock and rarefaction waves. Depending on the value p of the nonlinearity exponent, we find that both of these possibilities are realizable. We use a quasicontinuum approximation of a generalized inviscid Burgers model in order to predict the solution profile up to times near the formation of the dispersive shock, as well as to estimate when it will occur. Beyond that time threshold, oscillations associated with the highly dispersive nature of the underlying model emerge, which cannot be captured by the quasicontinuum approximation. Our analytical characterization of the above features is complemented by systematic numerical computations.

DOI: 10.1103/PhysRevE.95.062216

I. INTRODUCTION

Over the past two decades, the examination of granular crystals has received considerable attention, as is now summarized in a wide range of reviews [1–4] and popular articles [5]. Granular crystals consist of closely packed arrays of particles typically modeled as interacting with each other elastically via so-called Hertzian contacts. The resulting force depends on the geometry, contact angle, and elastic properties of the particles [6]. Part of the reason for the wide appeal of these systems is associated with their remarkable tunability, which permits one to access weakly or strongly nonlinear regimes. At the same time, it is possible to easily access and arrange the media in homogeneous or heterogeneous configurations. Notable examples of the latter include periodically arranged chains or those involving disorder. It is thus not surprising that granular crystals have been explored as a prototypical playground for a variety of applications including shock and energy absorbing layers [7–10], actuating devices [11], acoustic lenses [12], acoustic diodes [13,14], switches [15], and sound scramblers [13,16].

Much attention has been paid to special nonlinear solutions of the granular chain. Perhaps the most prototypical example explored in the context of granular crystals is the traveling solitary wave [1,2]. More recently, theoretical, computational, and experimental interests have been expanded to another broad class of solutions, so-called bright and dark discrete breathers, which are exponentially localized in space and periodic in time [3,5].

Our aim in the present work is to revisit a far less explored family of waveforms, namely, shock waves. The term shock wave can be interpreted in different ways, depending on the context (and the potential presence or absence of dissipation). In this paper and for the energy-conserving case examples considered herein, we characterize shock waves as states with an abrupt, nearly discontinuous change in the wave [17,18]. In the context of partial differential equations (PDEs), such as the inviscid Burgers equations, this definition can be made more precise to be a solution that develops infinite derivatives in finite time [19]. In dispersive media, the change in the medium occurs via a modulated wave train [17,18]. Such structures are called dispersive shocks. In experimental systems, dissipation can dominate the dispersion and the oscillations of the shock wave can be absent, as explored in [1,20]. Shock waves were studied experimentally in [21] by imparting velocity continuously to the end of a chain. More generally, in the context of the celebrated Fermi-Pasta-Ulam (FPU) lattices [22] (which bear significant similarities in their phenomenology to granular crystals in the presence of strong precompression), dispersive shock waves were examined numerically for the case of general convex FPU potentials for arbitrary Riemann (i.e., jump) initial data [23].

In this study we generalize the approach taken in the work of [24] (see also [25–27]). There it was recognized that the quasicontinuum form of the Hertzian model directly relates to a second-order PDE; for a rigorous justification, see [28]. Considering then the first-order nonlinear transport PDEs that represent the right- and left-moving waves, one retrieves effective models of the generalized family of the inviscid Burgers type [29]. This enables the use of characteristics in order to predict the evolution of initial data, as well as the potential formation of shock waves. We demonstrate that the formation of a dispersive shock in the granular chain without damping (highly dispersive medium) essentially coincides with the formation of a shock wave in the derived continuum model of the inviscid Burgers type.

The most commonly studied granular crystals are those consisting of strain-hardening materials. This implies that the nonlinear exponent satisfies $p > 1$ in $F \propto \delta^p$, where F and δ are compressive force and displacement. For example, in the Hertzian case of spherical particles, the nonlinear exponent is $p = 3/2$ [30]. More recently, generalizations of the Hertzian contact law have been explored in the context of mechanical metamaterials, including those with strain-softening behavior (where $0 < p < 1$) [31]. Examples of this include tensegrity structures [32] and origami metamaterial lattices [33,34]. Motivated by those recent works, we examine the formation of dispersive shock waves for general values of p. We find a fundamentally different dynamical behavior for the two cases

*Corresponding author: jkyang@aa.washingon.edu

of $p > 1$ and $p < 1$. For $p > 1$, for monotonically decreasing initial data, a dispersive shock forms due to the larger amplitudes traveling faster from the smaller ones. In the case of $p < 1$, the same initial data lead to a rarefaction waveform, where parts of the wave with small amplitude travel faster than larger-amplitude parts of the wave [35]. On time scales where the quasicontinuum approximation remains valid, we are able to analytically follow the solutions for both strain-hardening ($p > 1$) and strain-softening materials ($p < 1$). In the vicinity of the shock time (which we predict in reasonable agreement with the numerics from the quasicontinuum approximation), the discrete nature of the underlying lattice emerges and significantly affects the dynamics. Our systematic simulations illustrate, by varying quantities such as the precompression or the nonlinearity power, how these predictions become progressively less accurate as the model deviates from its linear analog.

Our presentation of the above results is structured as follows. In Sec. II we provide the theoretical background and analytical findings associated with the generalized model. In Sec. III we compare theoretical predictions to direct numerical simulations of the particle model. In Sec. IV we summarize our findings and present some possible directions for future work.

II. THEORETICAL ANALYSIS

Let u_n be the relative displacement from equilibrium of the nth particle in the lattice. As discussed in the Introduction, we are motivated by the generalization of the Hertzian contact model to arbitrary powers not only due to applications [32–34], but also due to significant theoretical developments (e.g., regarding traveling waves) [24,36,37]. In that light, we consider the following equation of motion:

$$\ddot{u}_n = [\delta_0 + u_{n-1} - u_n]_+^p - [\delta_0 + u_n - u_{n+1}]_+^p, \tag{1}$$

where δ_0 is the precompression (static load) applied to the system and the overdot represents differentiation with respect to normalized time. Defining the strain as $y_n = u_{n-1} - u_n$, we rewrite Eq. (1) as

$$\ddot{y}_n = (\delta_0 + y_{n-1})^p + (\delta_0 + y_{n+1})^p - 2(\delta_0 + y_n)^p. \tag{2}$$

Following [25] towards the derivation of a long-wavelength approximation characterized by the smallness parameter and the associated spatial and temporal scales $X = n$ and $T = t$, respectively, we express the strain as $y_n(t) = Y(X,T)$ and obtain

$$^2\partial_T^2 Y = \{\delta_0 + Y(X +)\}^p + \{\delta_0 + Y(X -)\}^p - 2\{\delta_0 + Y(X)\}^p.$$

Hence, the continuum model follows:

$$\partial_T^2 Y = \partial_X^2\{(\delta_0 + Y)^p\} + \frac{2}{12}\partial_X^4\{(\delta_0 + Y)^p\} + \cdots,$$

where the ellipsis denotes higher-order terms. If one considers long-wavelength solutions, then $\ll 1$ and thus the higher-order correction terms are ignored, resulting in the model

$$\partial_T^2 Y = \partial_X^2\{(\delta_0 + Y)^p\}. \tag{3}$$

Now, in the spirit of [29], consider the first-order (nonlinear transport) PDEs that would be compatible with Eq. (3),

$$\partial_T Y \pm \alpha\partial_X\{(\delta_0 + Y)^c\} = 0, \tag{4}$$

where $\pm$ indicates the two propagation directions. The parameters α and c will be chosen such that solutions of Eq. (4) are solutions of Eq. (3). From this we infer

$$\partial_T^2 Y = \partial_T[\mp\alpha\partial_X\{(\delta_0 + Y)^c\}] = \mp\frac{\alpha^2 c^2}{2c-1}\partial_X^2\{(\delta_0 + Y)^{2c-1}\}. \tag{5}$$

Comparing Eq. (3) and the right-hand side of the last equality of Eq. (5), we obtain $c = (p+1)/2$ and $\alpha^2 = \frac{2c-1}{c^2}$. Using these definitions of c and α, we rewrite Eq. (4) as

$$\partial_T Y \pm \sqrt{p}(\delta_0 + Y)^{(p-1)/2}\partial_X Y = 0. \tag{6}$$

Using then the standard technique of characteristics (see, e.g., [35] for an elementary discussion) in order to solve Eq. (6), we obtain the equation along characteristic lines (along which the solution is constant) of the form

$$\frac{dX}{dT} = \phi(Y(X,T)), \tag{7}$$

where

$$\phi(Y(X,T)) = \sqrt{p}[\delta_0 + Y(X,T)]^{(p-1)/2}. \tag{8}$$

Since solutions of Eq. (6) are constant along characteristic lines, Eq. (7) becomes

$$\frac{dX}{dT} = \frac{X - X_0}{T} = \phi(Y(X,T)) = \phi(Y(X_0,0)). \tag{9}$$

In this study we choose

$$Y_0(X_0) = a\,\mathrm{sech}(bX_0) \tag{10}$$

as the initial function, motivated by the interest in localized initial data.

As is well known in this broad class of generalized inviscid Burgers models, despite the smooth initial distribution of the strain y_n, a shock wave (a wave-breaking effect) can be observed to form in a finite time, i.e., the solution develops infinite derivatives in a finite time in the continuum limit of the problem [19]. This shock wave is created (due to the resulting multivaluedness) when the characteristic lines intersect. To predict when the shock wave is formed, i.e., the shock wave time T_s, we consider the two (arbitrary) characteristic lines

$$X(T) = \phi(X_1)T + X_1, \tag{11}$$

$$X(T) = \phi(X_2)T + X_2, \tag{12}$$

where $X_1, X_2 \in \mathbb{R}$ and $X_2 = X_1 + h$. When these two lines intersect we obtain

$$T = -\frac{X_2 - X_1}{\phi(X_2) - \phi(X_1)} = -\frac{h}{\phi(X_1 + h) - \phi(X_1)}. \tag{13}$$

The shock wave is formed at the time at which the characteristic lines intersect for the first time. Therefore, the shock time is calculated as follows:

$$T_s = \min\left[-\frac{h}{\phi(X_1 + h) - \phi(X_1)}\right] = \frac{1}{\min\left[-\frac{\phi(X_1+h)-\phi(X_1)}{h}\right]}.$$

Then, considering h 0, we obtain

$$T_s = -\frac{1}{\min\left[\frac{d\phi(X)}{dX}\right]}. \tag{14}$$

In this study our semianalytical prediction based on the above considerations consists of evaluating $\frac{d\phi(X)}{dX}$ and (numerically) identifying the relevant minimum, which leads via Eq. (14) to a concrete estimate of T_s to be compared with direct numerical simulations. It is also worth noting that as the time T_s of the shock formation is approached, the continuum approximation of Eq. (14) breaks down. Thus, in what follows, we will use the latter as a numerical diagnostic for the identification of T_s.

III. NUMERICAL COMPUTATIONS AND COMPARISON

Armed with the above theoretical considerations, we now turn to a comparison of the discrete model and the continuum model in terms of the formation of dispersive shock waves (as a way of quantifying the accuracy of our prediction). While true shock waves cannot form in the discrete system, it is reasonable to assume that the formation of a shock in the continuous model (3) coincides with the formation of a dispersive shock in the discrete model. This assumption is checked through the numerical simulations. In order to initialize the direct simulation of the discrete model, the initial velocity of each particle is needed.

Based on the initial strain $Y_0(X)$, the initial velocity that is consistent with the derivation of Eq. (3) can be computed as

$$\left[\frac{dy_n}{dt}\right]_{t=0} = \frac{d}{dt}[Y(X,T)]_{t=0}$$
$$= \pm\ [\sqrt{p}(\delta_0 + Y_0)^{(p-1)/2}\partial_X Y_0].$$

The initial strain is given by Eq. (10) with the numerical constants $a = 0.01$, $b = 0.3$, and $= 0.1$. These simulations will be compared to the continuum model approximations. The spatial profile of the continuum approximation at a given time t can be computed by solving the implicit equation

$$Y(\ n,\ t) = Y_0(\ n - \phi\ t), \tag{15}$$

where the wave velocity $\phi = \pm\ \sqrt{p(\delta_0 + Y(\ n,\ t))^{p-1}}$ follows directly from Eq. (6).

Figure 1 shows the strain wave propagation for the standard case of spherical Hertzian contacts $p = 1.5$ [1,2], while Fig. 2, motivated by the works of [32–34], shows the case of $p = 0.5$. Figures 1(a)–1(c) and 2(a)–2(c) show the wave shape at four different time instances and Figs. 1(d)–1(f) and 2(d)–2(f) show the space-time contour plots of strain wave propagation. In each case the top row represents the case of no precompression (fully nonlinear case), while progressively the middle and bottom rows introduce higher precompression, rendering the problem progressively more linear. For $p = 1.5$, the wave breaks from its front part (see Fig. 1), whereas the $p = 0.5$ case shows the wave breaking from the tail part, as shown in Fig. 2. This can be understood since the speed of propagation $\phi(Y(X,T))$ in the system depends on the amplitude of the wave [see Eq. (8)].

For $p > 1$, points along the initial condition with larger amplitudes travel faster than points with smaller amplitudes. Thus, the large-amplitude part of the wave overtakes the smaller amplitude part, leading to a dispersive shock formation in the front (monotonically decreasing part of the data) and a rarefaction in the back (monotonically increasing part of the data). On the contrary, for $p < 1$, the situation gets reversed, as is natural to infer from the speed expression $\phi(Y(X,T))$: The rarefaction forms in the front, while the wave breaking emerges in the back.

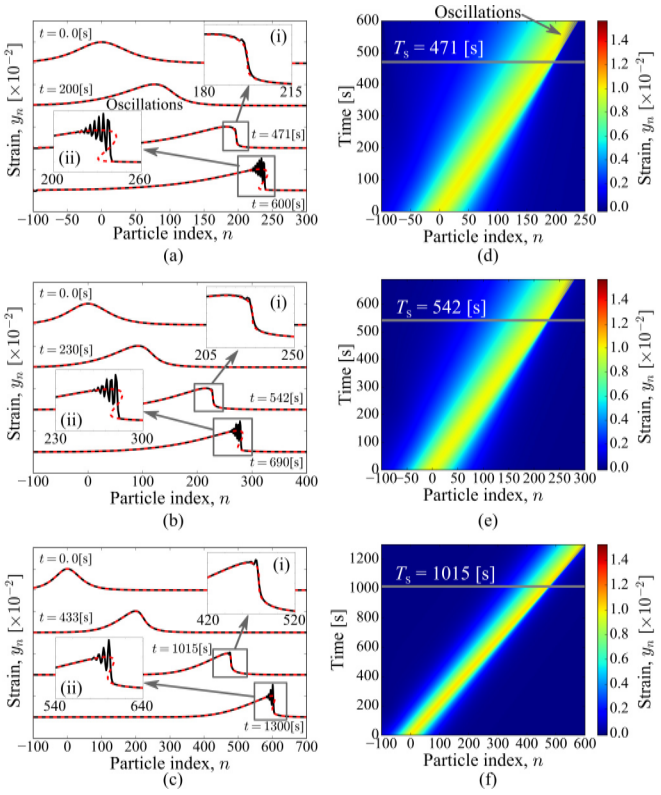

FIG. 1. Strain wave propagation for $p = 1.5$ and temporal plots of strain waves for (a) $\delta_0 = 0$, (b) $\delta_0 = 0.001$, and (c) $\delta_0 = 0.01$. The black solid line is obtained from the direct simulation of the discrete model and the red dashed line is the prediction based on Eq. (15) (i.e., the continuum model). Strain curves are offset to ease visualization (the tick interval in the vertical axis indicates 1.0). Insets (i) and (ii) show the magnified view of the leading part at and after the predicted shock time, respectively. Space-time contour plots of strain wave propagation for (d) $\delta_0 = 0$, (e) $\delta_0 = 0.001$, and (f) $\delta_0 = 0.01$. The gray solid line indicates the predicted analytical shock wave time.

In Figs. 1 and 2, in addition to showing the dynamics of the original underlying lattice of Eq. (1), the prediction based on the theoretical analysis of the nonlinear transport PDE is shown [see Eq. (15)]. It can be inferred that the two closely match *until* the time where a discontinuity is about to form, at which time the discrete model starts to feature oscillatory dynamics, a dispersive feature absent in the continuum long-wavelength model. A specific diagnostic in that connection that we use in order to compare the discrete and continuum cases is the shock formation time T_s. To obtain this time from the simulations, we examine the slope of the wave shape by calculating the sign of the differences of the strains between adjacent particles and we define the computational shock wave time T_s' when the sign changes multiple times, i.e., when the discrete character of the model prevents (the continuum) shock wave formation. The

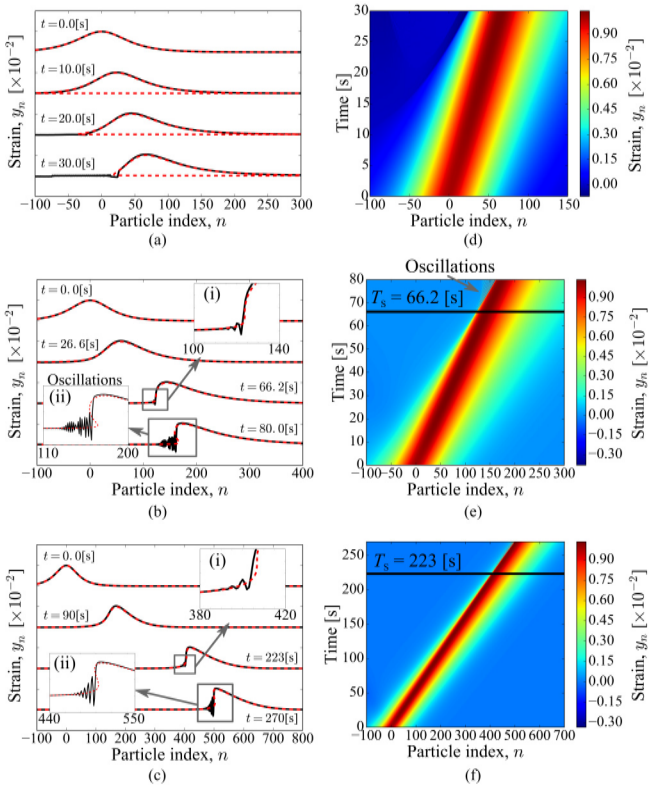

FIG. 2. Strain wave propagation for $p = 0.5$ and temporal plots of strain waves for (a) $\delta_0 = 0$, (b) $\delta_0 = 0.001$, and (c) $\delta_0 = 0.01$. The black solid line is obtained from the direct simulation of the discrete model and the red dashed line is the prediction based on Eq. (15) (i.e., the continuum model). Strain curves are offset to ease visualization (the tick interval in the vertical axis indicates 1.0). Insets (i) and (ii) show the magnified view of the tail part at and after the predicted shock time, respectively. Space-time contour plots of strain wave propagation for (d) $\delta_0 = 0$, (e) $\delta_0 = 0.001$, and (f) $\delta_0 = 0.01$. The black solid line indicates the predicted analytical shock wave time.

resulting comparison of T_s is a principal quantitative finding of the present work.

Figure 3 shows a comparison between numerical and analytical shock wave times for different exponent values p. The difference increases if p approaches unity because $p = 1$ indicates that the system becomes a linear advection equation, which does not support shock waves. It is for that reason that

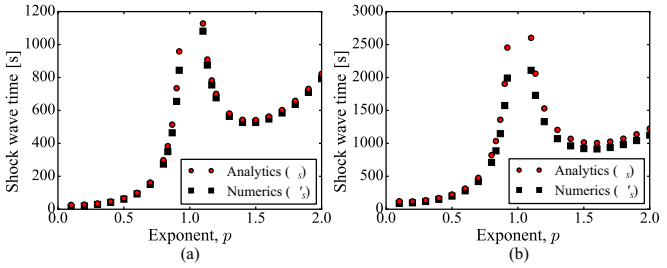

FIG. 3. Effect of the exponent value p on the shock wave time for (a) $\delta_0 = 0.001$ and (b) $\delta_0 = 0.01$. The red circles indicate the analytically predicted shock wave time (T_s), and the black squares denote the shock wave time from numerical simulations (T_s').

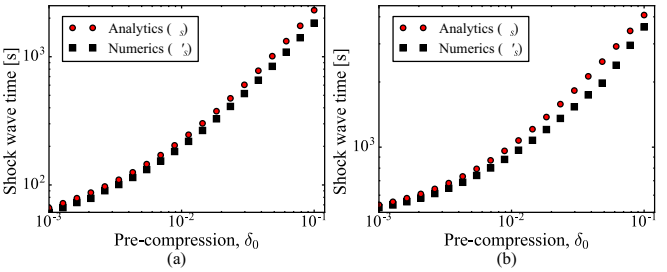

FIG. 4. Effect of the precompression δ_0 on the shock wave time for (a) $p = 0.5$ and (b) $p = 1.5$. The red circles indicate the analytically predicted shock wave time (T_s), and the black squares denote the shock wave time from numerical simulations (T_s'). Data are plotted on a log-log scale.

the shock formation time diverges as the limit p 1 is approached. Nevertheless, the quantitative trend between the two cases ($p > 1$ and $p < 1$) is well captured in both panels of the figure, i.e., for different values of the nonlinearity. In addition, we analyze the effect of precompression δ_0 on the shock wave time as shown in Fig. 4. As we increase the precompression (i.e., the system enters the weakly nonlinear regime and progressively approaches linear regime), the difference between numerical and analytical results increases. One can argue that this disparity may be partially related to the way we quantify the shock wave time. In particular, as the system approaches $p = 1$ or δ_0 large, linear modes become progressively more accessible to it (a situation to be contrasted with the sonic vacuum where no such modes exist). As a result, while in the sonic vacuum, in the effective absence of linear modes, the time of the shock nearly coincides with the emergence of nonmonotonicity near the wave front; in the progressively nearer linear case, the nonmonotonicity emerges earlier. Hence the numerical evaluation of T_s' (based on the emergence of discreteness induced oscillations) suggests that T_s' is calculated to be well before the wave-breaking event predicted by the analytics. Despite this distinction, it is fair to say that the quasicontinuum theory provides a very good tool for predicting the preshock wavefront evolution and for estimating the shock time, except in the vicinity of linear dynamical evolution.

IV. CONCLUSION AND FUTURE CHALLENGES

In the present work we investigated the emergence of dispersive shock and rarefaction wave formation in generalized granular crystal systems with Hertzian contacts. Motivated by recent developments in origami metamaterials [33,34] and tensegrity structures [32], we explored both the scenario of $p > 1$ (including $p = 3/2$ of spherical contacts) and that of $p < 1$ of strain-softening media. We identified the emergence of both dispersive shock waves and rarefaction waves and found a complementarity between the two cases. In the strain-hardening case, shock waves arise out of monotonically decreasing initial conditions and rarefactions out of monotonically increasing ones. The reverse occurs in the case of strain-softening $p < 1$ media. The generalization of the quasicontinuum formulation of [28] in the spirit of the nonlinear transport equations proposed in [29] provided us with an analytical handle in order to characterize the evolution

of pulselike data in the strain variables. A key quantitative prediction concerned the time of formation of the discontinuity as characterized at the quasicontinuum level. We discussed how the discreteness of the system, once visiting scales comparable to the lattice spacing, *intervenes* by generating oscillations and departing in this way from the quasicontinuum description.

This work suggests a number of exciting possibilities for the future. One interesting avenue is that of obtaining information about dispersive shock waves either at the level of the Korteweg–de Vries model or at that of the Toda lattice. Then, in the spirit of [38], we can use these to characterize the formation of dispersive shock waves that emerge in the presence of precompression. Nonetheless, it is unclear what becomes of such dispersive shock waves when precompression is weak or absent, as especially in the latter case there is no definitive characterization of dispersive shock waves. However, the direction of the first-order equations could be an especially profitable one in that context. The work of [39] (see also numerous references therein) suggests that for the inviscid Burgers problem shock waves have been extensively studied both analytically and numerically. It is conceivable that a (judiciously selected) discretization of the first-order PDEs considered herein could offer considerable insight into the formation of shock waves, both in the weak precompression and even in the case of the vanishing precompression limit. As demonstrated in [1,20], the presence of damping can change the dynamics significantly (where, e.g., the oscillatory nature of the shock is not observed) and thus extensions of this work that consider damping are also relevant.

ACKNOWLEDGMENTS

This material is based upon work supported by the National Science Foundation under Grant No. CAREER-1553202 and DMS-1615037. P.G.K. gratefully acknowledges support from the ERC under FP7; Marie Curie Actions, People, International Research Staff Exchange Scheme (Grant No. 605096); and the Alexander von Humboldt Foundation. J.Y. and P.G.K. are grateful for support from the ARO under Grant No. W911NF-15-1-0604.

[1] V. F. Nesterenko, *Dynamics of Heterogeneous Materials* (Springer, New York, 2001).
[2] S. Sen, J. Hong, J. Bang, E. Avalos, and R. Doney, Phys. Rep. **462**, 21 (2008).
[3] G. Theocharis, N. Boechler, and C. Daraio, in *Acoustic Metamaterials and Phononic Crystals* (Springer, Berlin, 2013), pp. 217–251.
[4] A. F. Vakakis, in *Wave Propagation in Linear and Nonlinear Periodic Media (International Center for Mechanical Sciences (CISM) Courses and Lectures)* (Springer, Berlin, 2012), p. 257.
[5] M. A. Porter, P. G. Kevrekidis, and C. Daraio, Phys. Today **68**(11), 44 (2015).
[6] K. L. Johnson, *Contact Mechanics* (Cambridge University Press, Cambridge, 1985).
[7] C. Daraio, V. F. Nesterenko, E. B. Herbold, and S. Jin, Phys. Rev. Lett. **96**, 058002 (2006).
[8] J. Hong, Phys. Rev. Lett. **94**, 108001 (2005).
[9] F. Fraternali, M. A. Porter, and C. Daraio, Mech. Adv. Mater. Struct. **17**, 1 (2010).
[10] R. Doney and S. Sen, Phys. Rev. Lett. **97**, 155502 (2006).
[11] D. Khatri, C. Daraio, and P. Rizzo, in *Nondestructive Characterization for Composite Materials, Aerospace Engineering, Civil Infrastructure, and Homeland Security 2008*, edited by P. J. Shull, H. F. Wu, A. A. Diaz, and D. W. Vogel, SPIE Proc. Vol. 6934 (SPIE, Bellingham, 2008), p. 69340U.
[12] A. Spadoni and C. Daraio, Proc. Natl. Acad. Sci. USA **107**, 7230 (2010).
[13] V. F. Nesterenko, C. Daraio, E. B. Herbold, and S. Jin, Phys. Rev. Lett. **95**, 158702 (2005).
[14] N. Boechler, G. Theocharis, and C. Daraio, Nat. Mater. **10**, 665 (2011).
[15] F. Li, P. Anzel, J. Yang, P. G. Kevrekidis, and C. Daraio, Nat. Commun. **5**, 5311 (2014).
[16] C. Daraio, V. F. Nesterenko, E. B. Herbold, and S. Jin, Phys. Rev. E **72**, 016603 (2005).
[17] M. J. Ablowitz and M. Hoefer, Scholarpedia **4**, 5562 (2009).
[18] G. A. El, M. A. Hoefer, and M. Shearer, SIAM Rev. **59**, 3 (2017).
[19] J. Smoller, *Shock Waves and Reaction-Diffusion Equations* (Springer, Berlin, 1983).
[20] E. B. Herbold and V. F. Nesterenko, Phys. Rev. E **75**, 021304 (2007).
[21] A. Molinari and C. Daraio, Phys. Rev. E **80**, 056602 (2009).
[22] E. Fermi, J. Pasta, and S. Ulam, Los Alamos Science Laboratory Report No. LA-1940 (1955) (unpublished); Reprinted in *Collected Papers of Enrico Fermi*, edited by E. Segre (University of Chicago Press, Chicago, 1965), Vol. 2, p. 978.
[23] M. Herrmann and J. D. M. Rademacher, Nonlinearity **23**, 277 (2010).
[24] K. Ahnert and A. Pikovsky, Phys. Rev. E **79**, 026209 (2009).
[25] M. A. Collins, Chem. Phys. Lett. **77**, 342 (1981).
[26] D. Hochstrasser, F. Mertens, and H. Büttner, Physica D **35**, 259 (1989).
[27] J. A. D. Wattis, J. Phys. A: Math. Gen. **26**, 1193 (1993).
[28] C. Chong, P. G. Kevrekidis, and G. Schneider, Discrete Contin. Dyn. Syst. A **34**, 3403 (2014).
[29] B. E. McDonald and D. Calvo, Phys. Rev. E **85**, 066602 (2012).
[30] H. Hertz, J. Reine. Angew. Math. **92**, 156 (1882).
[31] E. B. Herbold and V. F. Nesterenko, Phys. Rev. Lett. **110**, 144101 (2013).
[32] F. Fraternali, G. Carpentieri, A. Amendola, R. E. Skelton, and V. F. Nesterenko, Appl. Phys. Lett. **105**, 201903 (2014).
[33] H. Yasuda and J. Yang, Phys. Rev. Lett. **114**, 185502 (2015).
[34] H. Yasuda, C. Chong, E. G. Charalampidis, P. G. Kevrekidis, and J. Yang, Phys. Rev. E **93**, 043004 (2016).
[35] W. Strauss, *Partial Differential Equations: An Introduction* (Wiley, Hoboken, 2008).
[36] G. James and D. Pelinovsky, Proc. R. Soc. A **470**, 20130462 (2014).
[37] E. Dumas and D. E. Pelinovsky, SIAM J. Math. Anal. **46**, 4075 (2014).
[38] Y. Shen, P. G. Kevrekidis, S. Sen, and A. Hoffman, Phys. Rev. E **90**, 022905 (2014).
[39] C. V. Turner and R. R. Rosales, Stud. Appl. Math. **99**, 205 (1997).